

Kong-Shuang Zhao
Zhen Chen

An investigation on the high-frequency dielectric dispersion of concentrated ion-exchange resin beads suspensions

Received: 8 August 2005
Accepted: 21 January 2006
© Springer-Verlag 2006

K.-S. Zhao (✉) · Z. Chen
Department of Chemistry,
Beijing Normal University,
Beijing 100875,
People's Republic of China
e-mail: zhaoks@bnu.edu.cn

Abstract In this paper, dielectric measurements were carried out on concentrated suspensions of D₃₅₄ ion-exchange resin (IER) beads dispersed in electrolyte solutions. The distinct high-frequency dielectric behavior occurring in the megahertz frequency range was interpreted based on the understanding of the interparticle interaction and the properties of the constitute phases. The results indicated that the dominant parameter of continuous phase influencing HFDD is the

solution concentration after full Donnan equilibrium, while the dominant parameter of dispersed phase influencing HFDD is the fixed charge density. In addition, properties of the dispersed IER beads including electric conductivity and permittivity were obtained in terms of the Hanai's method.

Keywords High-frequency dielectric dispersion · Hanai's method · Ion-exchange resin beads · Donnan potential · Debye length

Introduction

Colloidal suspensions in electrolyte solutions exhibit a typical dielectric dispersion in the megahertz frequency range when subject to an oscillating electric field [1–9]. This phenomenon is generally called high-frequency dielectric dispersion (HFDD) or interfacial polarization dispersion. Maxwell [1] and Wagner [2] first studied this phenomenon and ascribed its mechanism to the well-known Maxwell–Wagner effect. This effect was later extended by O'Konski [3] by introducing the concept of surface conductivity. More recently, many researchers investigated HFDD in an electrokinetic way [4–9] and related it to many electrokinetic phenomena such as electrophoresis, making HFDD an effective tool in characterizing the electric double layer [10–13].

The theories about HFDD were developed based on dilute suspensions of insulating particles and have been applied fairly well to such systems. However, these theories will be confronted with difficulties and inaccuracy when applied to concentrated suspensions. Therefore, both theoretical and experimental investigations on HFDD of concentrated suspensions lag seriously behind those of

dilute suspensions nowadays. According to the works previously mentioned and many other works, we know the mechanism accounting for the HFDD of aqueous suspensions is due to the accumulation of ions in the particle–solution interface during the electromigration. While for concentrated suspensions, the presence of interparticle interaction enormously complicates this electromigration process. Nevertheless, the mechanism of HFDD for concentrated suspensions can be understood all the same by studying the interfacial electromigration process. In principle, this electromigration process is closely related to the properties of both the electrolyte solution and the particle; therefore, knowing the properties of both constituent phases for an actual suspension is very important in understanding the dispersion mechanism.

On the other hand, most experimental dielectric investigations were carried out for suspensions of well-defined particles [10–13], while suspensions of hard-to-define particles, such as charged porous particles and coated particles, are reported less frequently. In our present work, attention is paid to concentrated suspensions of charged porous particles. This kind of particles, for instance macroporous ion-exchange resin (IER) beads,

has some particular properties. First, while most insulating particles show noticeable surface conductivity when dispersed in aqueous solutions, the contribution of the surface conductivity for charged porous particles is negligible as compared to the bulk conductivity [14, 15]. Second, when particles of this kind are dispersed in a high-concentration electrolyte solution, some of their properties such as fixed charged density may be changed due to the ion exchange process. And third, as ionite particles, Donnan equilibrium is a basic phenomenon when they are dispersed in electrolyte solutions, and the Donnan potential ought to be one of the important parameters involved in many electrokinetic phenomena [14]. Although the properties of charged porous particles are hard to determine in many experiments, they can be conveniently determined in the HFDD experiments by means of Hanai's method [16, 17]. This method is based on the Wagner's equation [2] and the Hanai's equation [18] and was proven as rather practical in quantitatively relating the properties of constituent phases to the parameters that characterize the HFDD [15, 19].

In this paper, high-frequency dielectric measurements were carried out for the beads suspensions under different conditions. With the understanding of the interparticle interaction and the properties of the beads, the HFDD behaviors were discussed. Through these investigations, we tried to find out which parameters mainly influence the HFDD of this kind of suspensions and how these parameters work. It is hoped that these results can offer certain valuable information for the further theoretical development of HFDD.

Method and theory

Hanai's method

In Hanai's method [16, 17], the parameters that represent the properties of constituent phases and the suspension's conformation are defined as phase parameters, including κ_a , ε_i , κ_i , and φ . The parameters that characterize the dielectric behavior of HFDD are defined as dielectric parameters, such as ε_i , ε_h , κ_l , κ_h , and τ . Here, ε , κ , τ , and φ denote relative permittivity, electric conductivity, relaxation time, and volume fraction, respectively. The subscripts a, i, l, and h denote continuous phase, dispersed phase, limiting value at low (l) and high (h) frequency, respectively. The basic principle of the Hanai's method is the following: Now that the high-frequency dielectric behavior is essentially decided by the properties of both constituent phases, it is possible in principle to calculate phase parameters from dielectric parameters. For concentrated suspensions, the Hanai's method was recently presented in detail in Chen and Zhao [15] and Zhao et al. [19].

The Donnan equilibrium of the IER beads

The IER beads used in this work have porous configuration and contain positively charged groups fixed to the gel matrix [15]; hence, when the beads are in Donnan equilibrium with rather dilute electrolyte solutions (i.e., the fixed charge density is far bigger than the bulk salt concentration), the electrical conductivity κ_i can be expressed by the following approximate formulas for the limiting cases [20, 21]:

$$\kappa_i \approx X \lambda_-^i \quad (1)$$

where X is the fixed charge density, and λ_-^i is the equivalent anionic conductance in the resin beads whose value is smaller than in bulk solution [20–22]. While for insulating particles Zeta potential is an important parameter involved in HFDD, for IER beads the corresponding parameter is Donnan potential [14]. According to Ohshima and Kondo [23–25], the Donnan potential φ_D for an isolate ionite particle with thin double layer is equal to

$$\varphi_D = \frac{Z_f e N \lambda_D^2}{\varepsilon_a \varepsilon_0} \quad (2)$$

where Z_f and N are the valence and number density of fixed charge inside the sphere, respectively, ε_0 is the permittivity of a vacuum, e is the electric unit charge, and λ_D is the Debye length given by

$$\lambda_D = \sqrt{\frac{\varepsilon_a \varepsilon_0 k T}{e^2 \sum_i C_i Z_i^2}} \quad (3)$$

Here, k , T , C , and Z are Boltzmann constant, absolute temperature, number concentration, and valence of electrolyte solution.

Charge relaxation in bead–bead interacting region

The interacting region between two adjacent spherical particles is characterized by a characteristic length of the order of $(a \lambda_D)^{1/2}$ and a smallest distance of about $2 \lambda_D$, as illustrated by Fig. 7 in Lyklema et al. [26]. This region has important consequences for the surface charge polarization mechanism in it. For IER beads suspension, the field lines are locally perpendicular to the surface and the contribution of the surface conductance is negligible as compared to the volume conductance [15]; thus, the interfacial polarization relaxation processes mainly arise from the normal electromigration across the gap between interacting beads. When the added alternating field frequency is lower than the relaxation frequency (f_0), ions in the interacting region

have sufficient time to transport across the gap and then accumulate on the interface as polarized charges. Once the field frequency is higher than the relaxation frequency, ions there cannot have sufficient time to reach and accumulate on either interface but just keep oscillating for a very short distance. As a result, the relative permittivity of the whole system gradually decreases due to the continuous disappearance of polarized charges, while the electric conductivity of the whole system increases because of the additional oscillation of these ions. Because the gap is characterized by the Debye length, the relaxation time of HFDD is of the order of λ_D^2/D (D is the ion diffusivity), which is a manifestation of the Maxwell–Wagner’s theory. The relaxation amplitude of HFDD should be predicted by the magnitude of the polarized charges; thus, it should be a function of the amount of the charges involved in the interacting region.

Experimental

Materials and preparations of the suspensions

All the inorganic compounds used in our experiments were of analytical purity and used without further purification. The IER beads used here are the D₃₅₄ macroporous anion-exchange resin beads commercially available from Zheng-Guang Resin in HangZhou China, which corresponds to Amberlite IRA-93 in USA or WA-30 in Japan. The beads are 0.28 to 0.45 mm in diameter and contacting *tert*-ammonium group to macromolecule matrix of phenylethylene-vinylidene polymer. The beads used in “[Influences of continuous phase](#)” are in Cl-form, which were transformed by saturated NaCl solution by allowing the beads to be dispersed in saturated NaCl solution for at least 48 h. While in the experiments in “[Influences of dispersed phase](#),” the beads were transformed into four different forms: F-form, Cl-form, Br-form, and I-form, by being dispersed in 2 M solutions of NaF, NaCl, NaBr, and NaI, respectively. After transformation, the beads were washed by distilled water several times until the conductivities of the supernatants were reduced to the values of distilled water. Finally, the sediments of the beads were collected to dry in vacuum dryer for about 8 h.

Before dielectric measurement, copies of dried beads of equal weight were immersed in flasks with 50 ml corresponding solutions for 24 h, and when in dielectric measurement, the dielectric cell was charged with the electrodes being totally submerged in the slurry. The slurry actually consists of densely packed sediments of the IER beads in the aqueous phase.

Dielectric measurement

Dielectric measurements were carried out with an HP 4192A LF Impedance Analyzer from Hewlett-Packard at frequency ranging between 5 Hz and 13 MHz, which is controlled by a personal computer. The dielectric cell used in our study consists of concentric cylindrical platinum electrodes [27], and the cell constant and stray capacitance that have been determined by the use of several standard liquids were 0.25 and 1.26 pF, respectively. All experiments were carried out at 25 ± 0.5 °C, the pH values were kept to 7.3 ± 0.1 , and experimental data were all subjected to certain corrections [28] for the errors arising from residual inductance due to the cell assembly.

Electrode polarization correction and data treatment

Although electrode polarization effects are rather small in the frequency region of interest (over 10^5 Hz) [29], to obtain more reliable parameters, a generally used power-law frequency dependence method [29] was used to eliminate the electrode polarization effects. To correct, the following formula was applied:

$$\varepsilon_p = A \cdot f^{-b} \quad (4)$$

where ε_p is the equivalent permittivity arising from electrode polarization but superposed on the real experimental data, f is the frequency, and A and b are experimentally determined constants. When $\log \varepsilon_p$ is plotted against $\log f$, $\log \varepsilon_p$ will vary linearly over the low-frequency range where electrode polarization is dominant. Through this linear relationship, the constants A and b can be determined, thereby enabling the electrode polarization correction through subtraction of ε_p for each point of raw data.

Furthermore, a fitting-validation process was employed to ensure that both dielectric and phase parameters are the most reasonable. First, the well-known Cole–Cole equation [30] was used:

$$\varepsilon^* = \varepsilon_h + \frac{\varepsilon_l - \varepsilon_h}{1 + (i2\pi f)^\beta} \quad (5)$$

where ε^* is complex permittivity, i is $\sqrt{-1}$, f is the frequency, β is an experimental parameter denoting the width of the distribution of relaxation times around f_0 . When β equals to 1, the relaxation is the well-known Debye-type relaxation, and other symbols have the same meaning as introduced above. By separating the imaginary and real parts of ε^* , equations denoting the frequency dependences of relative permittivity and electric conductivity can be derived from Eq. 5, and the dielectric parameters can be obtained through fitting the dielectric

spectra in light of these equations. Then, the corresponding phase parameters can be calculated from the dielectric parameters by means of the Hanai's method introduced above. Since the phase parameters represent the properties of both constituent phases and suspension's conformation, we can simulate the theoretical curves by use of the phase parameters according to the Maxwell–Wagner theory [1, 2]. Finally, comparing the theoretical curves with the experimental ones, we can testify whether the phase parameters and, hence, the dielectric parameters, are reasonable or not. By doing so several times, we can find the most reasonable parameters for each suspension. Figure 1 is one of the results of this fitting-validation process, which corresponds to the suspension of IER beads dispersed in 0.2 mM NaCl solution. From Fig. 1, it can be seen that both the fitting curves and the theoretical curve are in good agreement with the experimental curve, indicating the validity of the parameters.

Results and discussion

Influences of continuous phase

There is no doubt that HFDD is closely related to the characteristics of the continuous phases even in highly concentrated suspensions. Basically, these characteristics include relative permittivity, solution viscosity, and properties of both coion and counterion. For the present suspensions where the continuous phases are dilute aqueous solutions, the relative permittivity and the solution viscosity will not vary obviously with different solutions, thus the characteristics that may remarkably influence HFDD are supposed to be the properties of the ions in the solutions. Because HFDD of concentrated suspension is mainly decided by the properties of the interacting region,

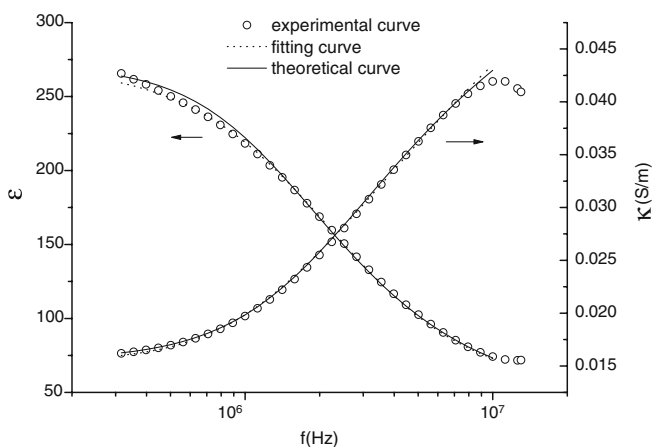


Fig. 1 A typical result of the fitting-validation process. Experimental, fitting, and theoretical curves of permittivity and electric conductivity as a function of frequency for suspension of IER beads in 0.2 mM NaCl solution

in which counterions play a predominant role while coions are thought to be negligible, the influence of the coions on HFDD is expected to be ignorable and that of counterions should be markedly. In view of that, dielectric measurements were carried out for two groups of suspensions. In group 1, Cl-form beads were dispersed in 0.2 mM solutions of NaCl, KCl, MgCl₂, CaCl₂, and AlCl₃, where the coion concentrations in all suspensions are equal. In group 2, Cl-form beads were dispersed in 0.8 mM NaCl, 0.8 mM KCl, 0.4 mM MgCl₂, 0.4 mM CaCl₂, and 0.8/3 mM AlCl₃ solutions, respectively, where the counterion concentrations in all suspensions are kept in equality.

Distinct dielectric dispersions were observed for both groups of suspensions at the frequency of the order of megahertz, as shown in Fig. 2a,b, which gives us the frequency dependences of the relative permittivity for the suspensions of group 1 and 2, respectively. It is easy to tell that these dielectric dispersions are HFDD according to the large particle radius but high relaxation frequency [15]. All the dielectric and phase parameters obtained by the fitting-validation process are listed in Table 1.

Most values of β listed in Table 1 are approximate to 0.9, which are considerably big and clearly indicate the presence of a single dispersion, considering that the beads suspensions are not actually monodisperse due to the distribution of the beads' radii. From Fig. 2a and the corresponding dielectric parameters listed in Table 1, we can clearly find that, although coion concentrations for all suspensions of group 1 are equal, the HFDD behaviors of these suspensions are apparently not all consistent. However, suspensions in equal counterion concentration have uniform dielectric behaviors including the relaxation amplitude ($\Delta\epsilon$) and the relaxation time (τ), examples are the one in 0.2 mM KCl solution and the one in 0.2 mM NaCl solution. It was reported [15, 19] that the amplitude of HFDD decreases as counterion concentration increases, which is true for the suspensions except for the one in AlCl₃ solution. The suspension in 0.2 mM AlCl₃ solution, which has the highest counterion concentration, unexpectedly exhibited the biggest relaxation in this group, looking more like an experimental accident. At the same time, it should be noted that the dielectric experiments on suspensions of group 2 give us similar results, except for the suspension in AlCl₃ solution, which also shows a surprisingly large HFDD. The other four suspensions exhibited uniform dielectric behavior as well, due to their equal counterion concentrations. If we leave the suspensions in AlCl₃ solutions alone, these results suggest well that the influence of coions on HFDD is negligible as compared with that of counterions, and the dielectric behaviors seem to be decided only by counterion concentration, making allowance for acceptable experimental errors. But why did the suspensions in AlCl₃ solutions behave so abnormally? We believe some exceptional mechanism happened when beads were dispersed in AlCl₃ solution, leading to some abnormal changes in both

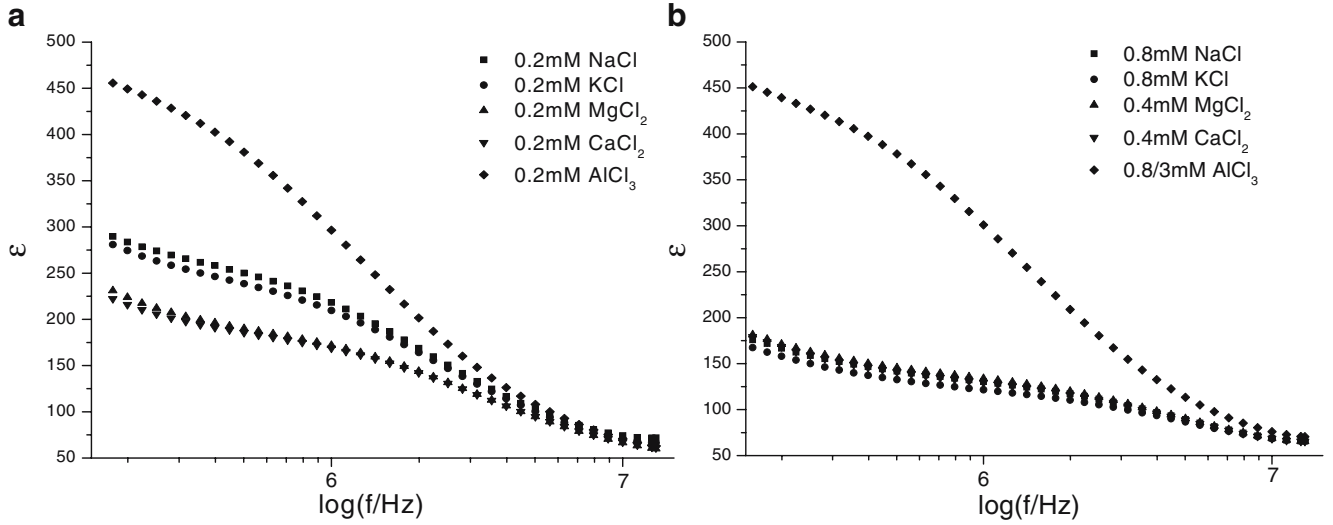


Fig. 2 Frequency dependences of relative permittivity for **a** the suspensions of Cl-form beads dispersed in 0.2 mM solutions of NaCl, KCl, MgCl₂, CaCl₂, and AlCl₃, respectively, and **b** the suspensions of Cl-form beads dispersed in solutions of 0.8 mM NaCl and KCl, 0.4 mM MgCl₂ and CaCl₂, and 0.8/3mM AlCl₃, respectively

constituent phases and eventually an unexpected dielectric behavior. To identify this mechanism, we should refer to the phase parameters that denote the properties of both constituent phases after beads being equilibrated with different electrolyte solutions.

From the phase parameters listed in Table 1, we can see that the values of the volume fraction lie around 0.53, which are reasonable values for monodisperse, closely packed sedimentary systems. As an ion-penetrable ionite particle, the IER bead in Donnan equilibrium with electrolyte solution is actually a combination of gel matrix and interstitial electrolyte solution. The relative permittivity ϵ_i , therefore, can be simply expressed by $\epsilon_i = f_w \epsilon_w + (1 - f_w) \epsilon_p$ [19], where f_w is the moisture content of the

beads, and ϵ_p and ϵ_w are the permittivity of the gel matrix and water. Basically, the relative permittivity of electrolyte solution is about 78 dielectric units and that of gel matrix is lower than 10. From these values, the moisture content of the beads is estimated to be 0.35, which is a reasonable value for this kind of IER beads. The values of κ_i are far bigger than those of κ_a , indicating that the fixed charge density is much bigger than the solution concentration. Therefore, κ_i is proportional to the fixed charge density according to Eq. 1. Since the beads have rigid structures, charge density remains fixed [14] and it is valid that the values of κ_i for all suspensions are equivalent. With the values of κ_a and of the equivalent ionic conductance of corresponding ions, the salt concentrations C_a of bulk

Table 1 Dielectric parameters, phase parameters, and solution concentrations for suspensions of Cl-form IER beads dispersed in different solutions

Specimen	Dielectric parameters						β	Phase parameters				
	ϵ_i	ϵ_h	$\Delta\epsilon$	κ_l (mS/cm)	κ_h (mS/cm)	τ (ns)		κ_a (mS/cm)	φ	ϵ_i	κ_i (mS/cm)	C_a (mM)
0.2 mM NaCl	273	50	223	0.156	0.514	73.0	0.877	0.0292	0.524	30.5	0.797	0.231
0.2 mM KCl	262	50	212	0.174	0.524	72.0	0.861	0.0324	0.524	31.1	0.796	0.216
0.2 mM MgCl ₂	192	50	142	0.225	0.540	51.5	0.911	0.0520	0.528	30.1	0.811	0.201
0.2 mM CaCl ₂	190	50	140	0.230	0.540	51.8	0.900	0.0529	0.522	30.8	0.800	0.195
0.2 mM AlCl ₃	476	45	431	0.070	0.505	122	0.836	0.00932	0.520	24.8	0.820	0.0223
0.8 mM NaCl	136	50	84	0.313	0.550	38.1	0.916	0.0887	0.529	31.9	0.804	0.702
0.8 mM KCl	127	51	72	0.332	0.556	36.1	0.900	0.0993	0.532	33.0	0.796	0.665
0.4 mM MgCl ₂	143	49	94	0.299	0.565	37.5	0.891	0.0821	0.544	31.1	0.798	0.318
0.4 mM CaCl ₂	136	49	87	0.316	0.574	36.3	0.895	0.0886	0.534	31.6	0.802	0.326
0.8/3 mM AlCl ₃	470	39	431	0.0792	0.576	112	0.818	0.0103	0.532	26.9	0.814	0.0246

ϵ Relative permittivity, κ electric conductivity, τ relaxation time, β the distribution of relaxation time, φ volume fraction of the beads, C_a solution concentration. Subscripts a, i, l, and h denote continuous phase, dispersed phase, limiting value at low (l) and high (h) frequency, respectively, and $\Delta\epsilon (= \epsilon_l - \epsilon_h)$ denotes dielectric increment

solutions after full equilibrium were obtained and are listed in Table 1. The values of C_a are different from those of the original electrolyte solutions, indicating that the presence of IER beads changed the solution concentration due to the absorption swelling process. It is noteworthy that the values of C_a of suspensions in AlCl_3 solution are extremely smaller than the corresponding pure solutions. This signifies that most Al^{3+} ions and Cl^- ions in bulk solution had transplanted to the beads when the beads were dispersed in AlCl_3 solution, either accumulating on the beads' surfaces or penetrating into them. In other words, most Al^{3+} ions were absorbed by the beads. This may be due to the special properties [31] of Al^{3+} ion such as high valence and small ionic radius and the excellent capability of absorption of this kind of beads. Once Al^{3+} ions were absorbed, Cl^- ions in the bulk solution also migrated to the beads so as to neutralize the beads, resulting in such a small solution concentration. This is why the suspensions in AlCl_3 solution behaved so abnormally. Judged by the values of κ_i , we can tell that most Al^{3+} ions only accumulated on the surface of beads but did not penetrate into them. If Al^{3+} ions could penetrate into the beads, the values of κ_i would have been apparently increased; however, the values were kept approximately equal to others.

As a conclusion, the relaxation time of present concentrated suspensions is mainly a function of the Debye length; hence, it is predicted by the solution concentration *after full equilibrium* according to Eq. 3, in line with Maxwell–Wagner's theory. The dielectric increment $\Delta\epsilon$, however, seems to be a function of the solution concentration as well. This because the interfacial charge distribution will adjust during particle encounter so as to maintain a constant potential (known as constant surface potential system) because the IER beads are ion-penetrable

[26]. The surface potential is basically decided by the Donnan potential for ion-penetrable surface [23–25]; therefore, dielectric increment of present suspensions is, in principle, a function of the Donnan potential now that it is decided by the amount of charges involved in the interacting region as aforementioned. Since the properties of beads are identical as shown in Table 1, $\Delta\epsilon$ is mainly a function of the Debye length according to Eq. 2.

Influences of dispersed phase

To investigate the influence of the dispersed phase, the beads were transformed into F-form, Cl-form, Br-form, and I-form, then dielectric experiments were carried out on suspensions of beads in different salt forms dispersed in 0.2 mM corresponding sodium halide solutions (suspensions of group 3); for instance, F-form beads were dispersed in 0.2 mM NaF solution. We did this to ensure only one kind of counterion involved in the relaxation process. As a comparison, dielectric experiments were also carried out on suspensions of Cl-form beads respectively dispersed in 0.2 mM NaF, NaCl, NaBr, and NaI solutions (suspensions of group 4). Fig. 3a,b respectively shows the frequency dependences of relative permittivity of suspensions of groups 3 and 4. By fitting the dielectric spectra, we obtained the dielectric parameters of all suspensions, from which the phase parameters were calculated by means of the Hanai's method. The dielectric and phase parameters are all listed in Table 2.

From Fig. 3b and the dielectric parameters listed in Table 2, we can see that the HFDD behaviors of the suspensions of group 4, including the relaxation amplitude and the relaxation time, are nearly consistent with one

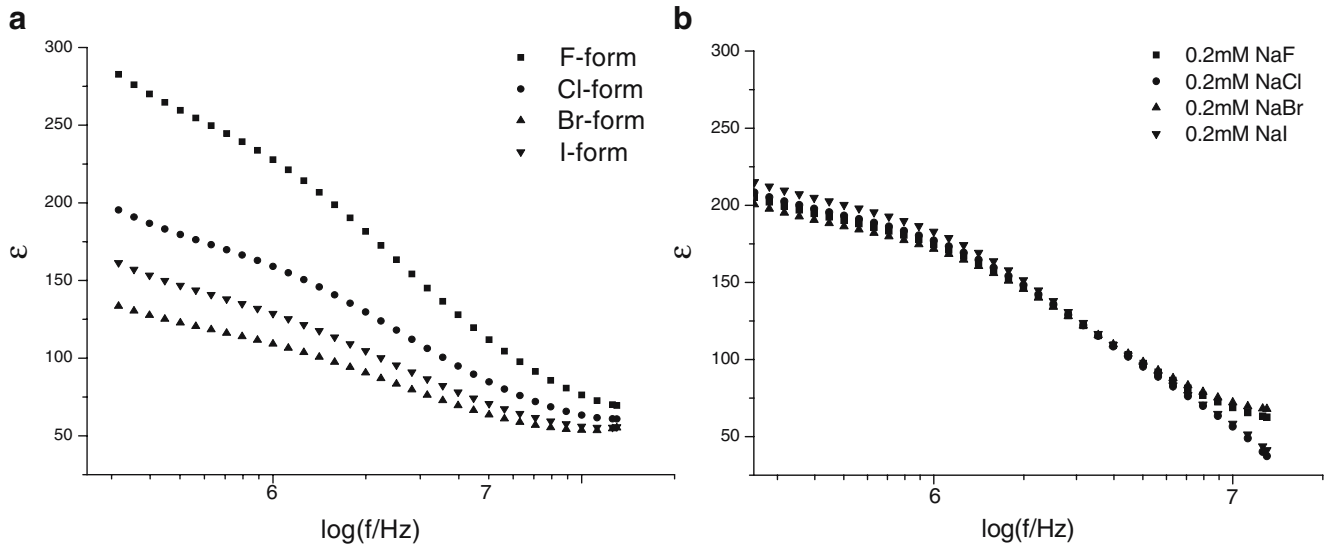


Fig. 3 Frequency dependences of relative permittivity of **a** suspensions of IER beads in different salt forms dispersed in 0.2 mM corresponding sodium halide solutions and **b** Cl-form IER beads dispersed in 0.2 mM different haloid solutions

Table 2 Dielectric parameters, phase parameters, and solution concentrations for suspensions of Cl-form IER beads, dispersed in 0.2 mM different haloid solutions, and IER beads in different salt forms dispersed in 0.2 mM corresponding haloid solutions

Specimen	Dielectric parameters						β	Phase parameters				
	ϵ_l	ϵ_h	$\Delta\epsilon$	κ_l (mS/cm)	κ_h (mS/cm)	τ (ns)		κ_a (mS/cm)	φ	ϵ_i	κ_i (mS/cm)	C_a (mM)
F-form in NaF	272	50	222	0.200	0.652	61.6	0.879	0.0374	0.532	30.8	0.986	0.354
Cl-form in NaCl	186	47	139	0.190	0.452	61.7	0.890	0.0438	0.528	27.6	0.652	0.346
Br-form in NaBr	126	40	86	0.159	0.314	62.1	0.884	0.0492	0.534	17.2	0.406	0.384
I-form in NaI	147	44	103	0.158	0.331	62.7	0.898	0.0443	0.526	22.2	0.456	0.343
Cl-form in NaF	197	48	149	0.211	0.544	50.4	0.896	0.0406	0.523	30.9	0.668	0.385
Cl-form in NaCl	198	47	151	0.209	0.552	50.1	0.899	0.0427	0.519	28.5	0.663	0.383
Cl-form in NaBr	196	47	150	0.212	0.549	50.2	0.865	0.0433	0.521	29.4	0.661	0.385
Cl-form in NaI	207	47	160	0.196	0.543	51.9	0.907	0.0395	0.513	28.9	0.654	0.347

ϵ Relative permittivity, κ electric conductivity, τ relaxation time, β the distribution of relaxation time, φ volume fraction of the beads, C_a solution concentration. Subscripts a, i, l, h denote continuous phase, dispersed phase, limiting value at low (l) and high (h) frequency, respectively, and $\Delta\epsilon(= \epsilon_l - \epsilon_h)$ denotes dielectric increment

another (the small discrepancies may arise from the tiny different solution concentration). This result implies that the properties of these haloid counterions themselves have little influence on HFDD. However, although the beads were dispersed in the same electrolyte solutions, the HFDD behaviors of suspensions of group 3 are distinctly different, as shown in Fig. 3a and the dielectric parameters in Table 2. This suggests that the properties of different salt form beads are different from one another, and the different properties can influence HFDD remarkably. Interestingly, from the dielectric parameters we can see that the relaxation times of suspensions of group 3 retain equivalence despite the different properties of the beads, suggesting that the relaxation time of HFDD have no bearing on the properties of the dispersed phase, at least for the present case.

For the suspensions of group 4, the phase parameters listed in Table 2 show that the properties of both constituent phases are equivalent. It should be noted that the values of the electric conductivity of the Cl-form beads retain approximately equal to 0.66 mS/cm, smaller than those of the Cl-form beads used in the previous section (0.80 mS/cm). This is apparently because the Cl-form beads used here are transformed by 2.0 M NaCl solution while those used in the previous section are transformed by saturated NaCl solution. For the suspensions of group 3, a similar result can be seen from the phase parameters. The beads in different salt forms have different electric conductivities, which is a result of the fact that the beads are transformed by different concentrations of haloid solutions. These results indicate that the properties of the IER beads can be changed when dispersed in thick electrolyte solutions. Now that the values of κ_i are still far bigger than those of κ_a for all suspensions here, κ_i is still proportional to X . The different values of κ_i indicate that the beads in different salt form have different fixed charge densities. From Table 2, we also noticed that the beads in different salt forms have different relative permittivities as well. This shows that the moisture content of beads in different salt form are

different: the beads that have higher moisture content allow more percent of electrolyte solution within the beads, leading to bigger bulk relative permittivities. In view of that, the moisture content of F-form beads is the highest and that of Br-form is the lowest. When more electrolyte solution exists in the beads, it is possible that more functional groups on the gel matrix will become active because of being exposed to external solution, giving rise to a bigger fixed charge density. Despite the different properties of the beads, the values of the volume fractions for all suspensions including those of groups 1 and 2 are maintained at around 0.53 too, which proves that the beads are rigid particles.

From the results above, we can conclude that the HFDD relaxation time of the present suspensions has no bearing on the properties of the dispersed phase, while the dielectric increment is still a function of the Donnan potential. Although the solution concentrations after full equilibrium and, hence, the Debye length are equal, the dielectric increment increases as the fixed charge density increases, which is consistent with Eq. 2.

Conclusion

By changing the properties of the continuous phase and the dispersed phase, high-frequency dielectric measurements were carried out for concentrated IER beads suspensions under different conditions. With the understanding of the particle–particle interaction and the properties of constitute phases, the HFDD behaviors of the suspensions in different conditions were interpreted, and the predominant parameters of each constitute phase that influence HFDD were discussed. The results showed that: (1) For the continuous phase, the primary parameter dominating HFDD is the solution concentration after full equilibrium, because it directly dominates the Donnan potential and the Debye length while the properties of coion and counterion

themselves have little influence on HFDD. (2) For the dispersed phase, the fixed charge density is the primary parameter dominating HFDD, since it principally decides the Donnan potential when the properties of the continuous phase are settled. However, the relaxation time of HFDD has no bearing on the properties of the dispersed phase. All in all, the HFDD relaxation time of the present suspension is predicted by the solution concentration after equilibrium, while the dielectric increment is predicted by the Donnan potential.

Besides, in terms of the Hanai's method, the properties of IER beads such as electric conductivity and permittivity were obtained, which are reasonable values for the present kind of beads. By analyzing the abnormal HFDD behaviors

of the suspensions in AlCl_3 solutions, we concluded that an adsorption process between Al^{3+} ions and the beads has happened when the beads were dispersed in AlCl_3 solutions, but this adsorption only happened on the surfaces of the beads rather than within them. As another successful example, this work once again proved the Hanai's method as a rather practical tool in obtaining the properties of constituent phases of a suspension by analyzing its high-frequency dielectric behaviors.

Acknowledgements Financial supports of this work by the National Natural Science Foundation of China (No: 20273010) are gratefully acknowledged.

References

1. Maxwell JC (1891) A treatise on electricity and magnetism, 3rd edn. Clarendon, Oxford
2. Wagner KW (1914) Arch Elektrotech 2:371
3. O'Konski CT (1960) J Chem Phys 64:605
4. Dukhin SS, Shilov VN (1974) Dielectric phenomena and the double layer in disperse systems and polyelectrolytes. Wiley, New York
5. O'Brien RW (1986) J Colloid Interface Sci 113:81
6. Grosse C (1988) J Phys Chem 92:3905
7. Dukhin SS (1995) Adv Colloid Interface Sci 61:17
8. Shilov VN, Delgado AV, González-Caballero F, Horno J, Lopez-García JJ, Grosse C (2000) J Colloid Interface Sci 232:141
9. Shilov VN, Delgado AV, González-Caballero F, Grosse C (2001) Colloids Surf A Physicochem Eng Asp 192:253
10. Blum G, Maier H, Sauer F, Schwan HP (1995) J Phys Chem 99:780
11. Grosse C, Tirado M, Pieper W, Pottel R (1998) J Colloid Interface Sci 205:26
12. Roldán-Toro R, Solier JD (2004) J Colloid Interface Sci 274:76
13. Jiménez ML, Arroyo FJ, Carrique F, Kaatz U, Delgado AV (2005) J Colloid Interface Sci 281:503
14. Grosse C, Shilov VN (1996) J Colloid Interface Sci 178:18
15. Chen Z, Zhao KS (2004) J Colloid Interface Sci 276:85
16. Hanai T, Ishikawa A, Koizumi N (1977) Bull Inst Chem Res Kyoto Univ 55:376
17. Hanai T, Imakita T, Koizumi N (1982) Colloid Polym Sci 260:1029
18. Hanai T (1960) Kolloid Z 171:23; Hanai T (1961) Kolloid Z 175:61
19. Zhao KS, Asami K, Lei JP (2002) Colloid Polym Sci 280:1038
20. Carstensen EL, Cox HA, Mercer WB, Natale LA (1965) Biophys J 5:289
21. Ishikawa A, Hanai T, Koizumi N (1984) Bull Inst Chem Res Kyoto Univ 62:251
22. Anderson JL, Quinn JA (1974) Biophys J 14:130
23. Ohshima H, Kondo T (1990) Biophys Chemist 38:117
24. Ohshima H, Kondo T (1990) J Colloid Interface Sci 140:291
25. Ohshima H, Kondo T (1993) J Colloid Interface Sci 155:499
26. Lyklema J, van Leeuwen HP, Minor M (1999) Adv Colloid Interface Sci 83:33
27. Hanai T, Zhang HZ, Sekine K, Asaka K, Asami K (1988) Ferroelectrics 86:191
28. Asami K, Irimajiri A, Hanai T, Koizumi N (1973) Bull Inst Chem Res Kyoto Univ 51:231
29. Schwan HP (1963) Physical techniques in biological research. Academic, New York
30. Cole KS, Cole RH (1941) J Chem Phys 9:341
31. Lee JM (1977) A new concise inorganic chemistry. Billing and Sons Guildford, London